ACS OMEGA
Open Access
http://pubs.acs.org/journal/acsodf
Article
This article is licensed under CC-BY-NC-ND 4.0

Novel Etch-Resistant Molecular Glass Photoresist Based on Pyrene Derivatives for Electron Beam Lithography

Xue Cong, Siliang Zhang, Jiaxing Gao, Xuewen Cui, Yurui Wu, Xudong Guo,* Rui Hu, Shuangqing Wang,* Jinping Chen, Yi Li, and Guoqiang Yang*

Cite This: *ACS Omega* 2024, 9, 37585−37595

Read Online

ACCESS | Metrics & More | Article Recommendations | Supporting Information

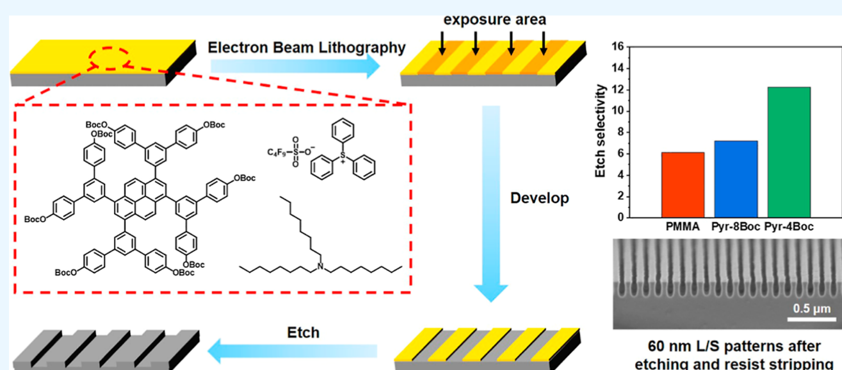

ABSTRACT: Novel *t*-butyloxycarbonyl-protected molecular glass photoresists with pyrene as the core (Pyr-8Boc and Pyr-4Boc) were designed and synthesized. The thermal stability and film-forming ability were measured to assess their applicability for lithography. Pyr-Boc (Pyr-8Boc and Pyr-4Boc) photoresists were evaluated by high-resolution electron beam lithography (EBL), acting as chemically amplified resists. Pyr-4Boc showed a better lithography performance, achieving 25 nm line/space patterns at the dose of 50 $\mu C/cm^2$. Under SF_6/O_2 plasma, the etch selectivity of the Pyr-4Boc photoresist to silicon was 12.3, which is twice that of the commercially available poly(methyl methacrylate) photoresist (950 k). The lithography mechanism of EBL was further investigated. Theoretical calculations of HOMO/LUMO orbital energies, cyclic voltammetry, and fluorescence quenching experiments were conducted to confirm the electron-transfer reactions between the Pyr-Boc and photoacid generator. The study provides an option of high sensitivity and etch-resistant photoresist for EBL.

INTRODUCTION

With the development of the semiconductor industry, the denser-integrated circuits and smaller crucial dimension (CD) are needed correspondingly as predicted in Moore's Law.[1,2] According to Rayleigh formula,[3] the resolution of CD is limited by the wavelength of optical lithography. The wavelength and lithography technologies have evolved from the initial g-line (436 nm) and i-line (365 nm) to 248 nm KrF and 193 nm ArF. The postoptical lithography, such as extreme ultraviolet (EUV), ion beam lithography, and electron beam lithography (EBL) are the most advanced lithography technologies for high resolution.[4−12] As the most important material in lithography, the performance of photoresists is directly related to the success of lithography. Ito et al. initially proposed chemical amplified resists (CARs) for 248 nm lithography.[13,14] The photoacid generators (PAGs) commonly used in these CARs are ionic iodonium salts and sulfonium salts,[15] which have strong 248 nm absorption. Although the stochastic defects and uncontrolled acid diffusion become significant when the CD required lower to sub-20 nm, considering of the trade-off of resolution, sensitivity, and line edge roughness (LER), CARs are still the largest class of photoresist materials used today due to the high sensitivity to afford high wafer throughput.[16,17] Research on this class of photoresist materials is ongoing, and attempts are being made to make further improvements in terms of increasing resolution,[18] reducing LER,[19] etc. Several research groups have conducted systematic reviews of this class of photoresists, and the results of these studies also serve as important references for this work.[15,20] Further improvement of the resolution without sacrificing LER and sensitivity by material design is also the direction of future research. In addition, when photoresists are exposed to electron beam or EUV light,

Received: February 1, 2024
Revised: August 14, 2024
Accepted: August 23, 2024
Published: August 27, 2024

ACS Publications
© 2024 The Authors. Published by American Chemical Society

https://doi.org/10.1021/acsomega.4c01044
ACS Omega 2024, 9, 37585−37595

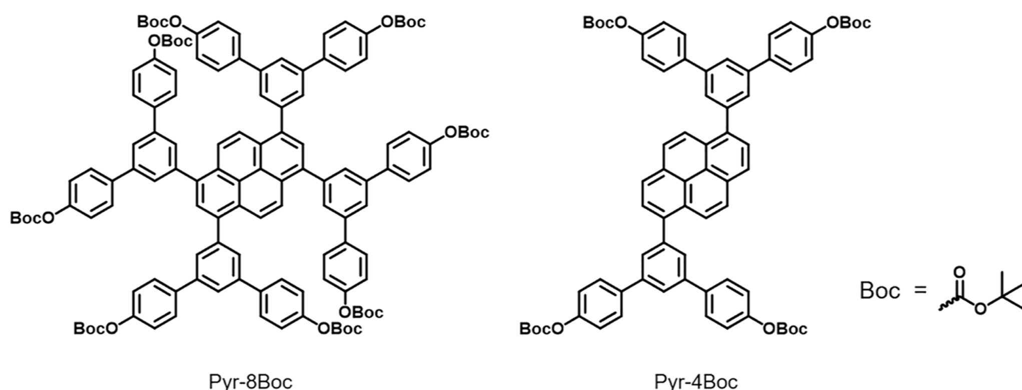

Figure 1. Chemical structures of Pyr-4Boc and Pyr-8Boc.

a cascade of reactions occurs in the exposure area, resulting in the generation of various types of reactive species.[21] Therefore, the lithography mechanism of CARs in EBL and EUV is indeed complex, and further exploration is still required. The study of the lithography mechanism will play an important role in promoting the development and application of new photoresists.

For advanced lithography, the photoresists are supposed to fulfill the requirements of high resolution, high sensitivity, low line width roughness (LWR) or LER. Due to the large-molecular weight and uneven distribution, traditional polymer photoresists face challenges in obtaining high resolution and low LER patterns. The molecular glasses with well-defined structures, small and monodisperse molecular weights, are beneficial for achieving high resolution and low LWR/LER patterns.[22−24] The slight modification of the cores or protecting groups can greatly affect the lithography performance. The selection of rigid and orthogonal conformation core with easily cleavable acid-labile groups is conducive to enhance the thermal properties, film formation, and sensitivity of photoresists. Several cores of molecular glasses have been reported, including bulky phenol derivatives,[25] fullerene derivatives,[26,27] and noria and calixarene derivatives.[28,29] These photoresists could achieve 25−32 nm L/S by EUV.[29] The synthesis and applications of the molecular glass photoresists have been previously reviewed by several research groups, and the conclusion is that this type of photoresist material will be a strong candidate for next generation of photoresist materials.[22,30,31] Based on t-butyloxycarbonyl (*t*-Boc) groups, our previous reports have developed bisphenol A derivatives,[32] 9,9′-spirobifluorene derivatives,[33] tetraphenylsilane derivatives,[34] and adamantane derivatives,[35,36] in which the resolution and LER were improved to 22 nm L/S and 3−4 nm LER, respectively. However, due to the low deprotection thermal activation energy, *t*-Boc groups could improve the sensitivity of photoresists while reducing the etching resistance, which greatly limits its application in photolithography.

After the patterns are precisely formed on the photoresist film, the etching process is conducted subsequently to transfer the patterns to the silicon substrate. Advanced lithography techniques require extremely thin photoresist films to minimize mechanical collapse of photoresists during development.[37] Thus, the high etch resistance performance of photoresist is necessary to ensure that it would not be totally consumed before the etching process is completed. The resistance of the photoresist to reactive ion etching is determined by the molecular structure. It was predicted that molecular organometallic resists exhibit significantly better etch selectivity than organic resists due to the introduction of the metal atom.[38] Some organometallic and coordinative photoresist materials containing Zr, Sn, Zn, and Fe have also been developed and achieved high resolution.[39−41] However, the introduction of metal may cause metal ion contamination, leading to failure of the integrated circuit.[42] In addition, several models based on empirical parameters have been established to predict the etching rate of organic photoresists, including Bond Contribution Model,[43] Ring Model,[44] and Ohnishi Model.[45] They revealed that the etching resistance can be improved by increasing the carbon content, the carbon atoms contained in the ring structure, carbon−carbon single bonds, and carbon−carbon double bonds in the structure of photoresists.[46,47] However, the commercially available photoresist in EBL, poly(methyl methacrylate) (PMMA), lacks cyclic structures, leading to poor etch resistance performance.

In this work, we reported two novel molecular glass photoresists based on pyrene derivatives with *t*-Boc groups protected (Figure 1). The core pyrene, linked to multiple benzene rings, provides etch resistance and thermal stability, while *t*-Boc acts as an acid-sensitive functional group to accomplish a dissolution transition at lower doses. The lithography performance and etch resistance of Pyr-Boc photoresists were evaluated by EBL and etching, respectively. They performed high sensitivity, resolution, and etch selectivity. The lithography mechanism of electron transfer was further investigated by cyclic voltammetry, DFT calculations, and fluorescence quenching experiments under 365 nm excitation.

■ EXPERIMENTAL SECTION

Instruments and Methods. The reagents and chemicals were purchased from commercial sources and used as received without any further purification. ^{1}H NMR spectra were measured with Bruker Fourier 300 MHz or Bruker AVANCE III 400 MHz at ambient temperature. $CDCl_3$ and DMSO-d_6 were used as solvents, and tetramethylsilane was used as the internal standard. The molecular weight was determined by a MALDI-FTICR-MS. Thermogravimetric analysis (TGA) was performed in a N_2 atmosphere with the heating rate of 10 °C/min from 30 to 500 °C. X-ray diffraction (XRD) curves of the powders were performed at room temperature.

Photoresist Film Preparation. The Pyr-Boc, triphenylsulfonium nonaflate (TPS-PFBS) (5 wt % of Pyr-Boc), and trioctylamine (10 wt % of PAG) were prepared and dissolved in propylene glycol methyl ether acetate (PGMEA) at a certain

https://doi.org/10.1021/acsomega.4c01044
ACS Omega 2024, 9, 37585−37595

Scheme 1. Synthesis of Compounds 1, 2, 3, 4, Pyr-8Boc and Pyr-4Boc

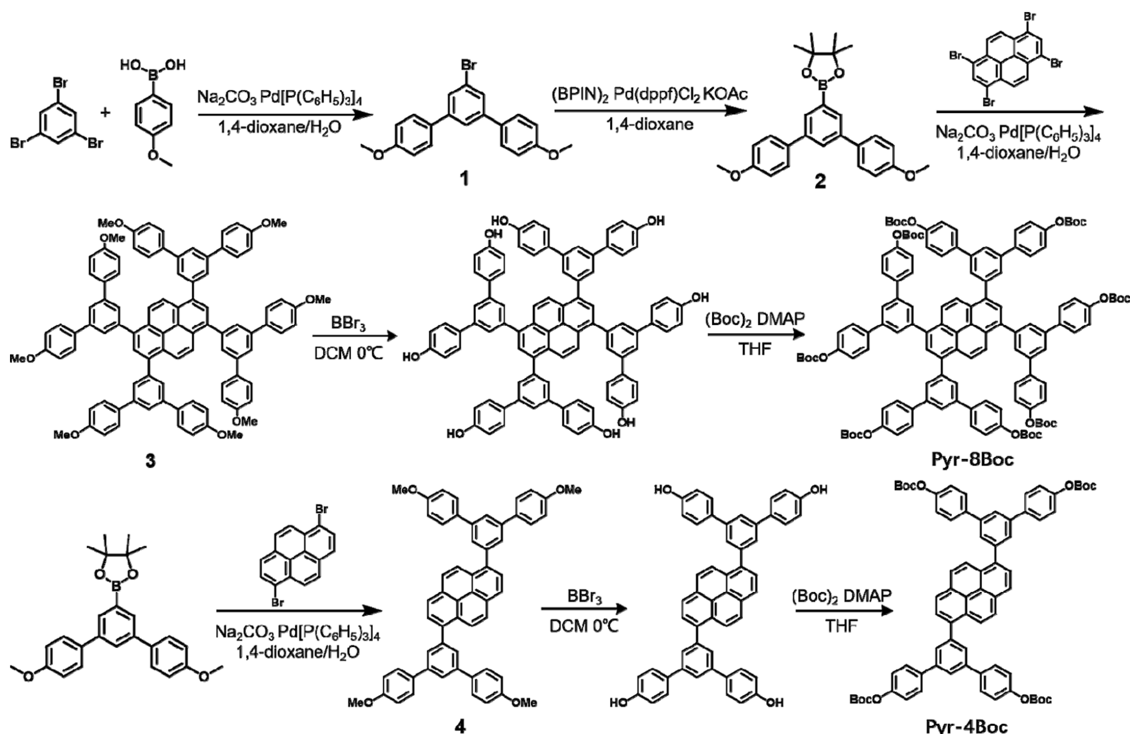

concentration. It should be noted that the formulations of photoresists have been optimized and selected to obtain a better photolithographic pattern in Supporting Information (Figure S1). The photoresist solution was filtered through a 0.2 μm membrane filter twice and spin-coated on a hexamethyldisiloxane primed silicon wafer with a CEE200X coating machine (Brewer Science CEE). Then, the prebake of 80 °C for 180 s on a hot plate was carried out to remove the solvent. The film thickness was measured by using an ASTSE200-BM spectroscopic ellipsometer (Angstrom Sun). Film roughness was estimated by using an atomic force microscope (AFM).

Electron Beam Lithography Performance. EBL patterning was performed by a Vistec EBPG 5000plus ES, using an exposure energy of 100 keV and a 100 pA beam current. After exposure, the postexposure bake was carried out at 90 °C for 30 s, then developed with 2.38 wt % tetramethylammonium hydroxide (TMAH) solution adding 1 mg/mL polyoxyethylene lauryl ether as a surfactant for 60 s (the surfactant polyoxyethylene lauryl was added to reduce the surface tension of water and increase the solubility of Pyr-Boc during development), and rinsed in pure water for 60 s before drying. The top-view and cross-sectional images were obtained by scanning electron microscopy (SEM) using a Hitachi Regulus 8230. The normalized remaining thickness (NRT) was measured by AFM. The LER was estimated by commercial ProSEM software.

Etching Resistance. An area of 0.5 × 0.5 μm^2 rectangular was exposed by EBL. The developed film on the silicon substrate was etched by a mixture plasma of SF_6/O_2 at −110 °C for 10 s on a Sentech/Etchlab200. After etching, the residual photoresist was removed by ultrasonic vibration in ethyl acetate and tetrahydrofuran for 1 min, respectively.

Photophysical and Electrochemical Properties. UV−vis absorption spectra were measured on a Hitachi U-3900H. The oxidation and reduction potentials were measured by cyclic voltammetry using a CHI660C instrument, with glassy carbon and Pt wire as the working and auxiliary electrodes, respectively. The reference electrode was Ag/AgCl (saturated KCl), and the supporting electrolyte was 0.1 M n-Bu_4NPF_6. A scan rate of 100 mV s^{-1} was carried out. The redox potential of ferrocene/ferrocenium (Fc/Fc^+) was measured for calibration. HOMO and LUMO energies of molecules were calculated by HOMO = $-(E_{ox} - E_{1/2}^{Fc^+/Fc} + 4.8)$ eV, LUMO = $-(E_{red} - E_{1/2}^{Fc^+/Fc} + 4.8)$ eV. The Gibbs free energy change ΔG_{et} of an electron-transfer reaction can be estimated from $\Delta G_{et} = E_{ox}(D/D^+) - E_{red}(A^-/A) - E^{00}$, where $E_{ox}(D/D^+)$, $E_{red}(A^-/A)$, and E^{00} are the oxidation of electron donor, the reduction of electron acceptor, and excitation energy of electron donor, respectively.

DFT Calculations of the HOMO/LUMO Orbital Energy. Gaussian 16 A.03 was used to calculate the HOMO/LUMO orbitals and energies.[48] Geometry optimizations and frequency calculations for Pyr-Boc and TPS-PFBS were performed using B3LYP/6-31G(d,p) and m062x/6-31G(d,p) level of theory with empirical dispersion correction DFT-D3(BJ), respectively.[49] Then, the single-point energies for Pyr-Boc and TPS-PFBS were calculated by B3LYP/def2TZVP and m062X/def2TZVP level of theory, respectively.[50,51]

Fluorescence Quenching. Fluorescence quenching experiments of Pyr-Boc were performed by using a Hitachi F-7100 fluorescence spectrometer with excitation at 365 nm. Concentrations from 0 to 9 mM of TPS-PFBS were added to the solution of 1 × 10^{-5} M Pyr-Boc.

RESULTS AND DISCUSSION

Synthesis and Characterization. The synthesis of Pyr-Boc is shown in Scheme 1. Pyr-4Boc and Pyr-8Boc both started from the Suzuki coupling of commercially available

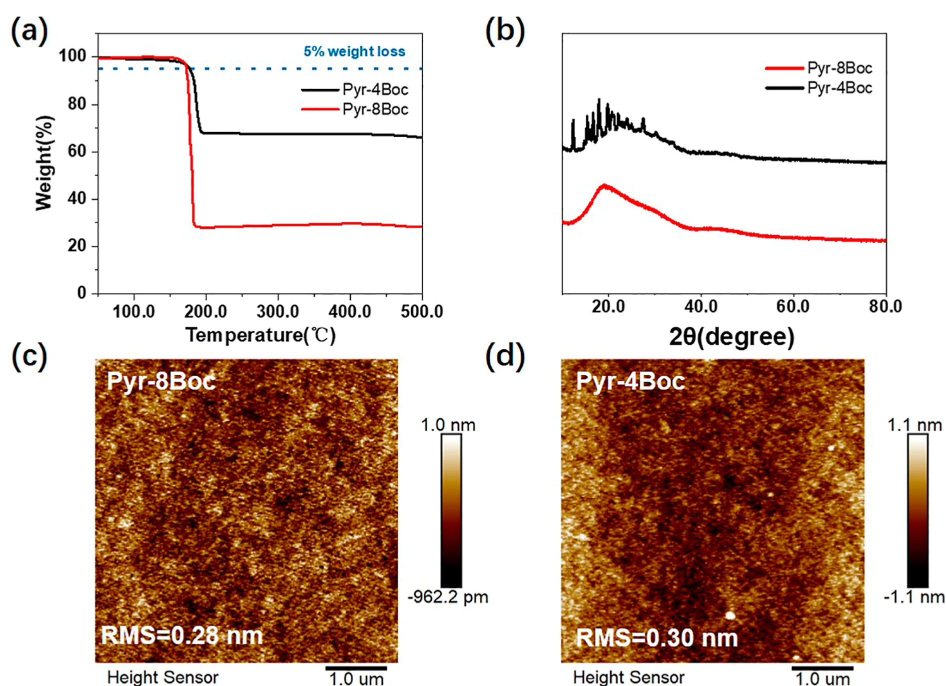

Figure 2. (a) TGA curves of Pyr-Boc; (b) XRD curves of Pyr-Boc; AFM images of (c) Pyr-8Boc and (d) Pyr-4Boc photoresist film.

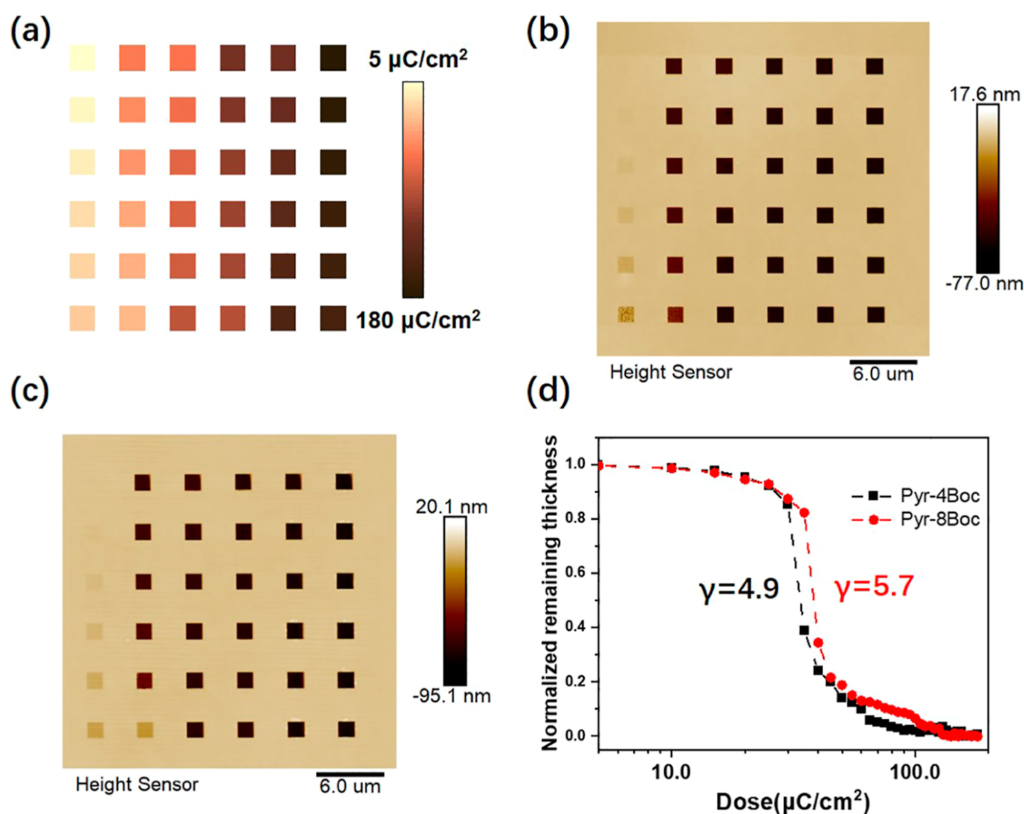

Figure 3. Sensitivity and contrast analysis of Pyr-Boc in EBL. (a) Electron beam exposure layout for NRT measurements. AFM images of (b) Pyr-4Boc and (c) Pyr-8Boc photoresist patterns developed with 2.38 wt % TMAH (adding 1 mg/mL polyoxyethylene lauryl ether) solutions. (d) Contrast curves of Pyr-4Boc and Pyr-8Boc.

tribromobenzene and 4-methoxyphenylboronic acid to give compound 1 in 58% yield. Miyaura-Ishiyama Borylation reaction of compound 1 and bis(pinacolato)diboron gave compound 2 in 91% yield. Then, Suzuki coupling between compound 2 with 1,3,6,8-tetrabromopyrene and 1,6-dibromopyrene was conducted, respectively, giving compounds 3 and 4 in 60 and 96% yields, respectively. The demethylation of compound 3 and followed by *t*-Boc protection reaction afforded the target compound Pyr-8Boc in a two-step yield of 49%. In a similar way, Pyr-4Boc was obtained in a two-step

https://doi.org/10.1021/acsomega.4c01044
ACS Omega 2024, 9, 37585−37595

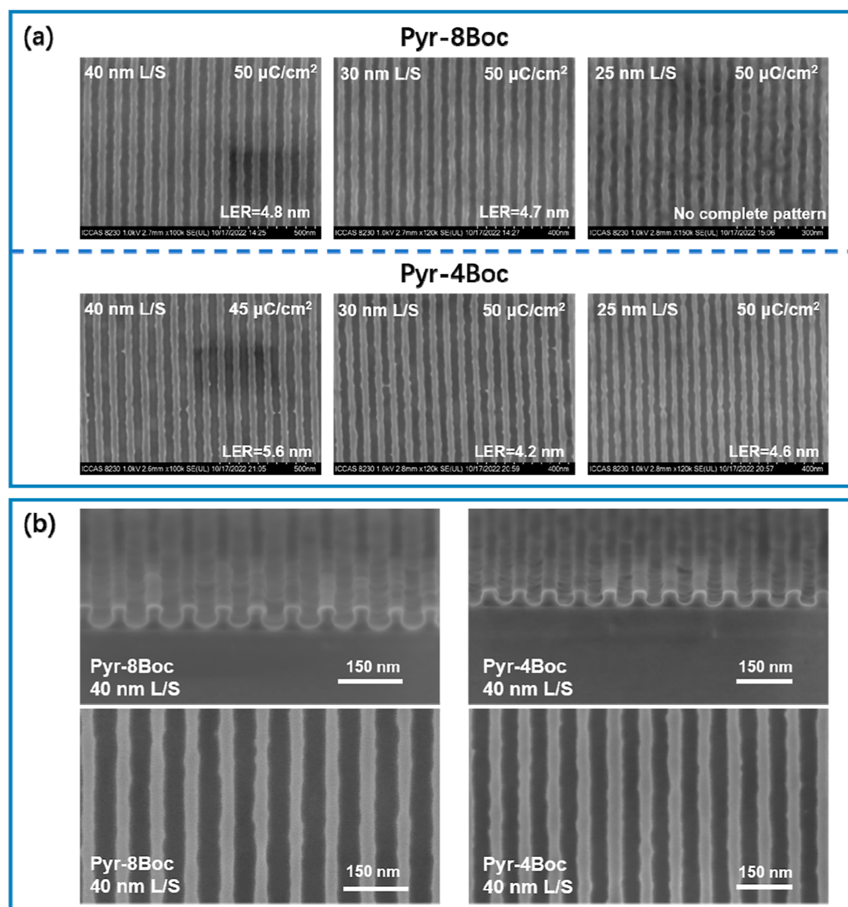

Figure 4. (a) SEM images of the patterns with 40, 30, and 25 nm L/S of Pyr-Boc photoresists (film thickness: 34−36 nm) at the dose of 45−50 $\mu C/cm^2$; (b) cross-section and corresponding top-down patterns of dense lines/space of HP 40 nm for the Pyr-8Boc photoresist (film thickness: 78 nm) and Pyr-4Boc photoresist (film thickness: 62 nm).

reaction of 63%. Details of the synthesis process are provided in our previous report,[52] the synthesized Pyr-8Boc and Pyr-4Boc are evaluated in Supporting Information (Figures S2−S5).

Thermal Behaviors and Film Forming Performance. The thermal stability of Pyr-Boc was characterized by TGA (Figure 2a). The initial decomposition temperature for Pyr-8Boc and Pyr-4Boc is 172 and 176 °C, respectively. It proves that Pyr-Boc photoresists can meet the needs of lithography, in which the process of soft bake and postexposure bake require the photoresist to be stable at baking temperature (90 °C).

It is important to ensure that the surface of the photoresist film is uniform and free of particle defects; high crystallinity is not conducive to the formation of high-quality films. The XRD curves for Pyr-Boc show a broad central peak at $2\theta = 20°$, and the curve is smoother for Pyr-8Boc (Figure 2b), indicating the amorphous state of Pyr-8Boc and some microcrystallinity of Pyr-4Boc. This may be attributed to the less stereoscopic structure of Pyr-4Boc, but it obviously does not affect their uniform film formation obviously. The root-mean-square (RMS) roughness of the Pyr-8Boc and Pyr-4Boc films was estimated as 0.28 and 0.30 nm in an area of 5×5 μm^2 (Figure 2c,d), respectively, suggesting that they are suitable for film formation and high-resolution lithography.

EBL Performance of Pyr-8Boc and Pyr-4Boc Photoresists. The sensitivity and contrast of Pyr-Boc in EBL were investigated by measuring the remaining film thickness after development at different exposure doses. Contrast (γ) is defined as the slope in the NRT curves by eq 1[53]

$$\gamma = \left|\log\left(\frac{D_2}{D_1}\right)\right|^{-1} \quad (1)$$

For positive photoresists, D_2 is the minimum dose required to remove the photoresists totally; D_1 is the maximum dose at which the thickness of the photoresist remains constant. As shown in Figure 3a, 36 square patterns (1.5 μm × 1.5 μm) were exposed on the photoresist film, with the dose starting at 5 $\mu C/cm^2$ and gradually increasing at a step of 5 $\mu C/cm^2$. Then, the thicknesses of the exposed and developed patterns were measured (Figure 3b,c). Figure 3d shows the contrast curves of Pyr-Boc, and the sensitivity and contrast of Pyr-4Boc are 46 $\mu C/cm^2$ and 4.9, respectively, and 50 $\mu C/cm^2$ and 5.7 for Pyr-8Boc, respectively.

The capability of forming 1:1 line/space (L/S) patterns of the Pyr-Boc photoresists is shown in Figure 4a. To minimize mechanical collapse in small pitch patterns, 34−36 nm film thickness was chosen. For Pyr-8Boc photoresist, the 40 and 30 nm L/S patterns were obtained at the dose of 50 $\mu C/cm^2$, and the LER parameters were calculated as 4.8 and 4.7 nm, respectively. However, there are some obvious collapses and breaks in the 25 nm half pattern (HP). Compared to Pyr-8Boc, Pyr-4Boc achieves a higher resolution, the 40, 30, and 25 nm L/S patterns were observed at the dose of 45−50 $\mu C/cm^2$,

https://doi.org/10.1021/acsomega.4c01044
ACS Omega 2024, 9, 37585−37595

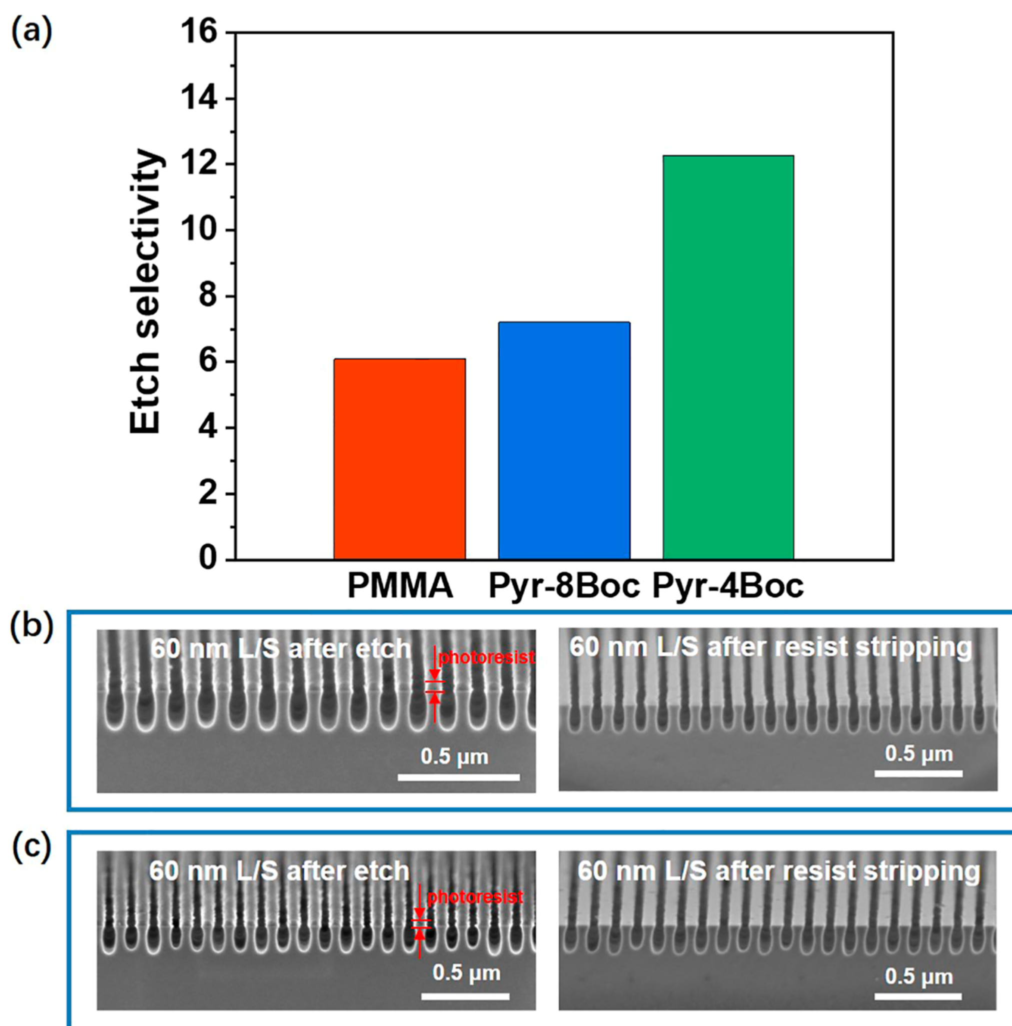

Figure 5. Measurements of etch selectivity and pattern transfer capability. (a) Etch selectivity to silicon of the PMMA (950 k), Pyr-8Boc, and Pyr-4Boc photoresists. The cross-section patterns of dense lines/space of HP 60 nm after etching and resist stripping for (b) Pyr-4Boc and (c) Pyr-8Boc photoresists.

with 4, 4.2, and 4.6 nm LER, respectively. Details of the LER calculations are provided in Supporting Information in Figures S6 and S7. The larger film thickness facilitates the assessment of the steepness of the Pyr-Boc photoresist sidewall profile; therefore, cross-sectional and corresponding top-down images of lithographic patterns of 40 nm L/S lines with 60−80 nm thickness were investigated (Figure 4b). Both Pyr-8Boc and Pyr-4Boc can achieve steep sidewalls without top-rounding, and there is almost no residue in the trench, although some footing was observed.

Etch Resistance and Pattern-Transfer Capability of Pyr-Boc Photoresists. The relationship between the molecular structure of photoresist and the etching rate can be described by the Ohnishi Model,[45] as shown in eq 2

$$V \propto \frac{N_T}{N_C - N_O} \quad (2)$$

where V, N_T, N_C, and N_O are the etching rate, total number of atoms in a molecule, the number of carbon atoms, and the number of oxygen atoms, respectively. According to the Ohnishi Model, it can be assumed that the proportionality constant is the same, and the etching rate ratio of PMMA,[45] Pyr-8Boc, and Pyr-4Boc is calculated to be 2:1.04:1. The developed photoresist film on the silicon substrate was etched by a mixture plasma of SF_6/O_2, it was found that Pyr-8Boc showed an etch selectivity to silicon of 7.2, and Pyr-4Boc showed an etch selectivity of 12.3, which is twice that of the commercial electron beam photoresist, PMMA (950 k) (Figure 5a). Details of film thicknesses after development, etching, and resist stripping are provided in Supporting Information Figures S8−S10, respectively. Pyr-4Boc exhibits a higher etch resistance than Pyr-8Boc due to its larger percentage of carbon atoms in the molecular structure. Furthermore, cross-section patterns of 60 nm L/S after etching and resist stripping for Pyr-Boc photoresists are shown in Figure 5b,c. The 60 nm HP patterns were transferred accurately to the silicon wafer with an aspect ratio at 2.5:1. Due to the isotropy of the etching process, the transferred pattern showed a distinct concave profile, which can be improved by adding an underlayer on the wafer.

Electron-Transfer Reactions between Pyr-Boc and PAG. In EBL, the photoresist matrix absorbs the high percentage of the radiation energy instead of the PAG due to its majority in CAR composition.[54] Thus, the decomposition pathway of PAG becomes different from that of photolytic reactions. The common mechanism involves

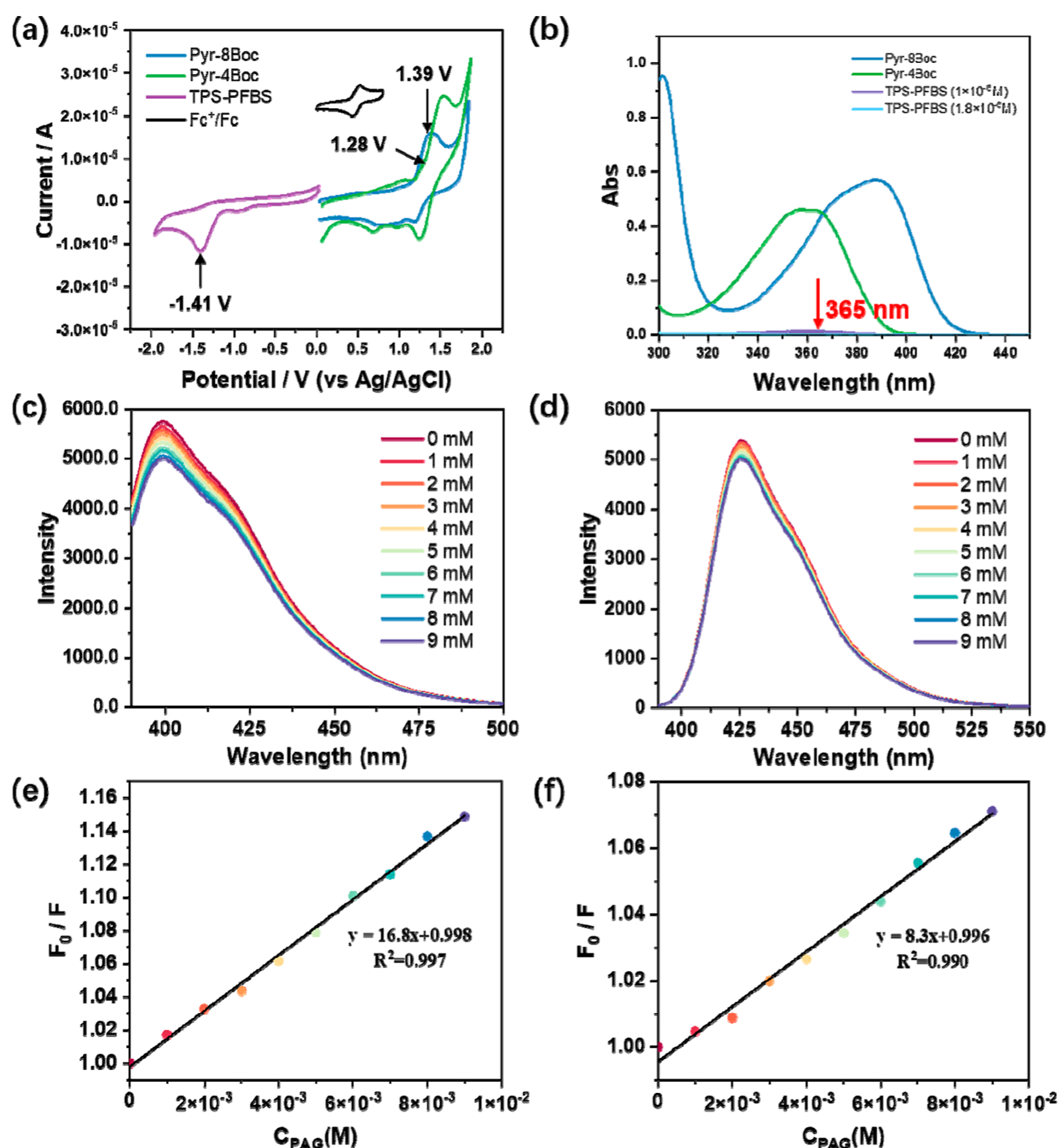

Figure 6. (a) Cyclic voltammogram of Pyr-8Boc, Pyr-4Boc, TPS-PFBS, and ferrocene in anhydrous dichloromethane solution at room temperature; (b) UV/vis absorption spectra of Pyr-8Boc (1×10^{-5} M), Pyr-4Boc (1×10^{-5} M), and TPS-PFBS (1.8×10^{-6} M and 1×10^{-6} M, which is 5 wt % of Pyr-8Boc and 5 wt % of Pyr-4Boc, respectively) in PGMEA; fluorescence emission quenching of (c) Pyr-4Boc (1×10^{-5} M) and (d) Pyr-8Boc (1×10^{-5} M) by adding different concentrations of TPS-PFBS from 0 to 9 mM, λ_{ex} = 365 nm; Stern−Volmer plots (e) for Pyr-4Boc and (f) for Pyr-8Boc.

ionization of the photoresist matrix, the generation of secondary electrons and radical cations, the electron transfer between photoresist matrix and PAGs, the deprotonation of photoresist matrix, and the subsequent acid amplification reactions.[55,56] In this work, conventional experimental methods were used to illustrate the electron-transfer process, which has rarely been tested in previous studies.

The redox behaviors of Pyr-8Boc, Pyr-4Boc, and TPS-PFBS in solution were investigated by cyclic voltammetry (Figure 6a). The first oxidation waves of Pyr-8Boc and Pyr-4Boc were estimated at E_p^{ox} = 1.39 V and E_p^{ox} = 1.28 V (vs Ag/AgCl), respectively, and the first reduction wave of TPS-PFBS was observed at E_p^{red} = −1.41 V (vs Ag/AgCl). Thus, the HOMO energies of Pyr-8Boc and Pyr-4Boc were calculated as −5.71 and −5.6 eV, respectively, and the LUMO energy of TPS-PFBS was calculated as −1.25 eV. It indicates that Pyr-4Boc is a better electron donor than Pyr-8Boc, in agreement with the calculations of Gaussian 16 A.03 (Supporting Information Figure S11). Based on these results, free energy change ΔG_{et} of the electron-transfer reaction, in which Pyr-4Boc and Pyr-8Boc as the electron donor and TPS-PFBS as an electron acceptor were determined to be −0.73 and −0.4 eV, respectively. This means that Pyr-Boc can undergo an electron-transfer process with TPS-PFBS.

Both Pyr-4Boc and Pyr-8Boc show absorption at around 365 nm (Figure 6b), whereas PAG TPS-PFBS is transparent in this region. This suggests that TPS-PFBS is unable to undergo photoinduced decomposition by absorbing photons and reaching the excited state when exposed to 365 nm light. Under excitation at 365 nm, the fluorescence emission intensity of Pyr-Boc decreased with the presence of varying concentrations of TPS-PFBS in PGMEA (Figure 6c,d). The fluorescence quenching process can be described by the classical Stern−Volmer eq 3[57]

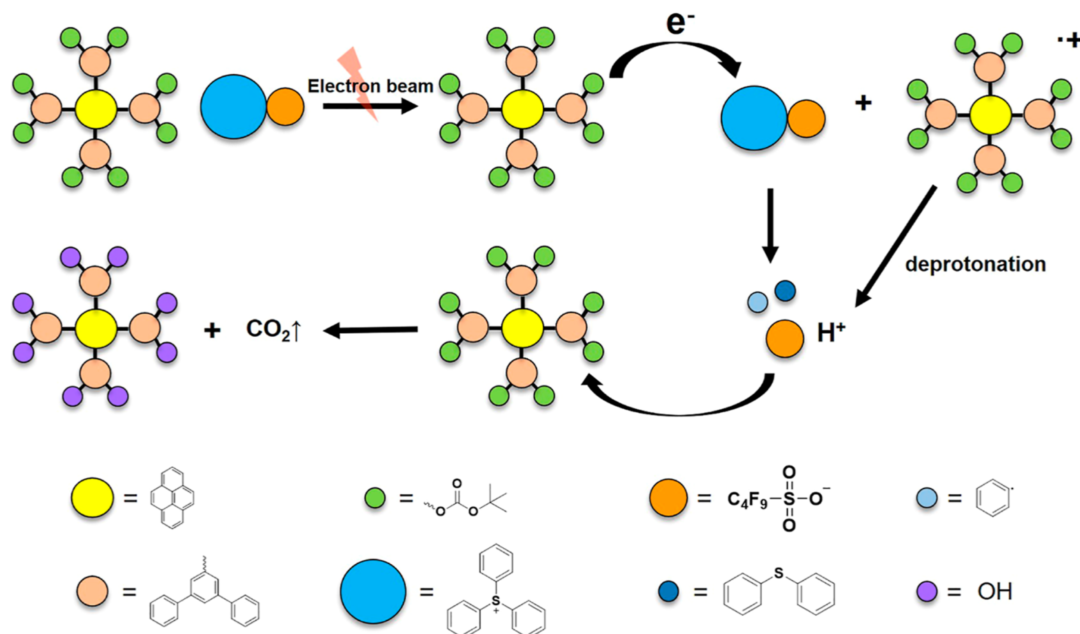

Figure 7. Summary of the lithography mechanism of Pyr-Boc photoresists in EBL.

$$\frac{F_0}{F} = 1 + K_D[Q] \tag{3}$$

where F_0 and F are the fluorescence intensities in the absence and the presence of the quencher, respectively; Q is the concentration of quencher, and K_D stands for the Stern–Volmer quenching constant. The linear relationship was found in F_0/F and concentration of PAG (Figure 6e,f), and K_D was calculated to be 16.8 for Pyr-4Boc and 8.3 for Pyr-8Boc, respectively. The fluorescence emission quenching experiments indicate the deactivation of excited state Pyr-Boc by electron transfer, proving that the electron-transfer reaction between Pyr-Boc and TPS-PFBS has taken place. In addition to using 365 nm ultraviolet light excitation, the pathway for Pyr-Boc to reach the excited state can also occur during EBL under high energy electron irradiation, and then the excited state of Pyr-Boc can undergo electron transfer with the PAG.

Proposed Lithographic Mechanism of Pyr-Boc Photoresists in EBL. Based on the aforementioned results and previous literature,[58,59] a possible mechanism of electron beam exposure was proposed (Figure 7). Under electron beam irradiation, Pyr-Boc acts as a sensitizer for TPS-PFBS, undergoing ionization processes and transferring electrons to TPS-PFBS, in which the electron-transfer process has been validated using specific experimental methods. Then, the radical cation of Pyr-Boc donates protons to TPS-PFBS through deprotonation. The cation part of TPS-PFBS acts as an electron acceptor and decomposes,[59,60] and the anion part obtains protons to form photoacid, which in turn catalyzes the deprotection reaction of *t*-Boc groups in Pyr-Boc, releasing carbon dioxide, and producing phenol hydroxyl groups. After alkaline water development, the exposed area is removed, leaving the unexposed area to form patterns.

CONCLUSIONS

In summary, two molecular glass photoresists based on pyrene derivatives with *t*-Boc protecting groups have been synthesized (i.e., Pyr-4Boc and Pyr-8Boc), both of which have good thermal and film-forming abilities and are suitable as positive photoresists in EBL. Using Pyr-4Boc in EBL can achieve a higher resolution (HP 25 nm) with a high sensitivity (50 μC/cm^2) and contrast (4.9). The Pyr-Boc photoresists exhibit high etch resistance, in which the etch selectivity of Pyr-4Boc is twice that of commercial PMMA photoresists (950 k). The electron-transfer reactions between the Pyr-Boc and the PAG were detected by conventional experimental methods. The validation of the electron-transfer reaction mechanism enables the explanation of possible reactions during the EBL process. These results show that Pyr-Boc photoresists are compelling candidates for applications in high-resolution EBL with improved performance.

ASSOCIATED CONTENT

Supporting Information

The Supporting Information is available free of charge at https://pubs.acs.org/doi/10.1021/acsomega.4c01044.

Optimization of photoresist formulation; characterizations of Pyr-Boc; LER measurements of SEM images; etch selectivity of Pyr-Boc and PMMA (950 k); and DFT calculations of the HOMO/LUMO of Pyr-8Boc, Pyr-4Boc and TPS-PFBS (PDF)

AUTHOR INFORMATION

Corresponding Authors

Xudong Guo − *Beijing National Laboratory for Molecular Sciences, Key Laboratory of Photochemistry, Institute of Chemistry, Chinese Academy of Sciences, University of Chinese Academy of Sciences, Beijing 100190, China;* orcid.org/0000-0002-2012-4399; Email: scoopguo@iccas.ac.cn

Shuangqing Wang − *Beijing National Laboratory for Molecular Sciences, Key Laboratory of Photochemistry, Institute of Chemistry, Chinese Academy of Sciences, University of Chinese Academy of Sciences, Beijing 100190, China;* orcid.org/0000-0002-8281-9399; Email: g1704@iccas.ac.cn

Guoqiang Yang − *Beijing National Laboratory for Molecular Sciences, Key Laboratory of Photochemistry, Institute of Chemistry, Chinese Academy of Sciences, University of Chinese Academy of Sciences, Beijing 100190, China;* orcid.org/0000-0003-0726-2217; Email: gqyang@iccas.ac.cn

Authors

Xue Cong − *Beijing National Laboratory for Molecular Sciences, Key Laboratory of Photochemistry, Institute of Chemistry, Chinese Academy of Sciences, University of Chinese Academy of Sciences, Beijing 100190, China*

Siliang Zhang − *Beijing National Laboratory for Molecular Sciences, Key Laboratory of Photochemistry, Institute of Chemistry, Chinese Academy of Sciences, University of Chinese Academy of Sciences, Beijing 100190, China*

Jiaxing Gao − *Beijing National Laboratory for Molecular Sciences, Key Laboratory of Photochemistry, Institute of Chemistry, Chinese Academy of Sciences, University of Chinese Academy of Sciences, Beijing 100190, China*

Xuewen Cui − *Beijing National Laboratory for Molecular Sciences, Key Laboratory of Photochemistry, Institute of Chemistry, Chinese Academy of Sciences, University of Chinese Academy of Sciences, Beijing 100190, China*

Yurui Wu − *Beijing National Laboratory for Molecular Sciences, Key Laboratory of Photochemistry, Institute of Chemistry, Chinese Academy of Sciences, University of Chinese Academy of Sciences, Beijing 100190, China*

Rui Hu − *Beijing National Laboratory for Molecular Sciences, Key Laboratory of Photochemistry, Institute of Chemistry, Chinese Academy of Sciences, University of Chinese Academy of Sciences, Beijing 100190, China;* orcid.org/0000-0003-4949-6214

Jinping Chen − *Key Laboratory of Photochemical Conversion and Optoelectronic Materials, Technical Institute of Physics and Chemistry, Chinese Academy of Sciences, University of Chinese Academy of Sciences, Beijing 100190, China;* orcid.org/0000-0002-5632-2290

Yi Li − *Key Laboratory of Photochemical Conversion and Optoelectronic Materials, Technical Institute of Physics and Chemistry, Chinese Academy of Sciences, University of Chinese Academy of Sciences, Beijing 100190, China;* orcid.org/0000-0002-7018-180X

Complete contact information is available at: https://pubs.acs.org/10.1021/acsomega.4c01044

Notes

The authors declare no competing financial interest.

■ ACKNOWLEDGMENTS

This work was supported by the National Natural Science Foundation of China (22073108, 22090012, U20A20144, 22275198, and 22375209) and the Youth Innovation Promotion Association of Chinese Academy of Sciences (2020035). We also thank the National Center for Nanoscience and Technology of China for EBL experiments and etching experiments.

■ REFERENCES

(1) Pirati, A.; Schoot, J.; Troost, K.; Ballegoij, R.; Krabbendam, P.; Stoeldraijer, J.; Loopstra, E.; Benschop, J.; Finders, J.; Meiling, H.; Setten, E.; Niclas, M.; Dredonx, J.; Stamm, U.; Kneer, B.; Thuering, B.; Kaiser, W.; Heil, T.; Migura, S. The future of EUV lithography: enabling Moore's Law in the next decade. *Proc. SPIE* **2017**, *10143*, 101430G.

(2) Golio, M. Fifty Years of Moore's Law [Scanning Our Past]. *Proc. IEEE* **2015**, *103*, 1932−1937.

(3) Prabhu, V. M.; Kang, S.; VanderHart, D. L.; Satija, S. K.; Lin, E. K.; Wu, W. L. Photoresist latent and developer images as probed by neutron reflectivity methods. *Adv. Mater.* **2011**, *23*, 388−408.

(4) Naulleau, P.; Anderson, C. N.; Baclea-an, L.-M.; Chan, D.; Denham, P.; George, S.; Goldberg, K. A.; Hoef, B.; Jones, G.; Koh, C.; Fontaine, B. L.; McClinton, B.; Miyakawa, R.; Montgomery, W.; Rekawa, S.; Wallow, T. The SEMATECH Berkeley MET pushing EUV development beyond 22nm half pitch. *Proc. SPIE* **2010**, *7636*, 76361J.

(5) Putna, E. S.; Younkin, T. R.; Leeson, M.; Caudillo, R.; Bacuita, T.; Shah, U.; Chandhok, M. EUV lithography for 22nm half pitch and beyond: exploring resolution, LWR, and sensitivity tradeoffs. *Proc. SPIE* **2011**, *7969*, 76962K.

(6) Gao, J.; Zhang, S.; Cui, X.; Cong, X.; Guo, X.; Hu, R.; Wang, S.; Chen, J.; Li, Y.; Yang, G. Effective Optimization Strategy for Electron Beam Lithography of Molecular Glass Negative Photoresist. *Adv. Mater. Interfaces* **2023**, *10*, 2300194.

(7) Ito, T.; Okazaki, S. Pushing the limits of lithography. *Nature* **2000**, *406*, 1027−1031.

(8) Lewis, S. M.; DeRose, G. A.; Alty, H. R.; Hunt, M. S.; Lee, N.; Mann, J. A.; Grindell, R.; Wertheim, A.; De Rose, L.; Fernandez, A.; Muryn, C. A.; Whitehead, G. F. S.; Timco, G. A.; Scherer, A.; Winpenny, R. E. P. Tuning the Performance of Negative Tone Electron Beam Resists for the Next Generation Lithography. *Adv. Funct. Mater.* **2022**, *32*, 2202710.

(9) Yogesh, M.; Moinuddin, M. G.; Chauhan, M.; Sharma, S. K.; Ghosh, S.; Gonsalves, K. E. Organoiodine Functionality Bearing Resists for Electron-Beam and Helium Ion Beam Lithography: Complex and Sub-16 nm Patterning. *ACS Appl. Electron. Mater.* **2021**, *3*, 1996−2004.

(10) Wang, Z.; Chen, J.; Yu, T.; Zeng, Y.; Guo, X.; Wang, S.; Allenet, T.; Vockenhuber, M.; Ekinci, Y.; Yang, G.; Li, Y. Sulfonium-Functionalized Polystyrene-Based Nonchemically Amplified Resists Enabling Sub-13 nm Nanolithography. *ACS Appl. Mater. Interfaces* **2023**, *15*, 2289−2300.

(11) Wang, Y.; Chen, J.; Zeng, Y.; Yu, T.; Wang, S.; Guo, X.; Hu, R.; Tian, P.; Vockenhuber, M.; Kazazis, D.; Ekinci, Y.; Wu, Y.; Yang, S.; Zhao, J.; Yang, G.; Li, Y. Nonchemically Amplified Molecular Resists Based on Sulfonium-Functionalized Sulfone Derivatives for Sub-13 nm Nanolithography. *ACS Appl. Nano Mater.* **2023**, *6*, 18480−18490.

(12) Liu, Q.; Zhao, J.; Guo, J.; Wu, R.; Liu, W.; Chen, Y.; Du, G.; Duan, H. Sub-5 nm Lithography with Single GeV Heavy Ions Using Inorganic Resist. *Nano Lett.* **2021**, *21*, 2390−2396.

(13) Ito, H.; Willson, C. G. Chemical amplification in the design of dry developing resist materials. *Polym. Eng. Sci.* **1983**, *23*, 1012−1018.

(14) Ito, H. Chemical amplification resists: history and development within IBM. *IBM J. Res. Dev.* **1997**, *41*, 119−130.

(15) Goldfarb, D. L. Evolution of patterning materials towards the Moore's Law 2.0 Era. *Jpn. J. Appl. Phys.* **2022**, *61*, SD0802.

(16) Peng, X.; Wang, Y.; Xu, J.; Yuan, H.; Wang, L.; Zhang, T.; Guo, X.; Wang, S.; Li, Y.; Yang, G. Molecular Glass Photoresists with High Resolution, Low LER, and High Sensitivity for EUV Lithography. *Macromol. Mater. Eng.* **2018**, *303*, 1700654.

(17) Ongayi, O.; Wood Ii, O. R.; Christianson, M.; Meyer, M.; Coley, S.; Valeri, D.; Kwok, A.; Wagner, M.; Cameron, J.; Thackeray, J. High sensitivity chemically amplified EUV resists through enhanced EUV absorption. *Proc. SPIE* **2012**, *8322*, 83220T.

(18) Yang, D.; Chang, S. W.; Ober, C. K. Molecular glass photoresists for advanced lithography. *J. Mater. Chem.* **2006**, *16*, 1693−1696.

(19) Tarutani, S.; Tsubaki, H.; Fujimori, T.; Takizawa, H.; Goto, T. Novel EUV Resist Materials Design for 14 nm Half Pitch and below. *J. Photopolym. Sci. Technol.* **2014**, *27*, 645−654.

(20) Manouras, T.; Argitis, P. High Sensitivity Resists for EUV Lithography: A Review of Material Design Strategies and Performance Results. *Nanomaterials* **2020**, *10*, 1593.
(21) Wang, Q.; Zhou, Y.; Wang, X.; Gao, H.; Shu, Z.; Hu, Z.; Tao, P.; Ekinci, Y.; Vockenhuber, M.; Chen, Y.; Duan, H.; Xu, H.; He, X. Suppressing of secondary electron diffusion for high-precision nanofabrication. *Mater. Today* **2023**, *67*, 95−105.
(22) Li, L.; Liu, X.; Pal, S.; Wang, S.; Ober, C. K.; Giannelis, E. P. Extreme ultraviolet resist materials for sub-7 nm patterning. *Chem. Soc. Rev.* **2017**, *46*, 4855−4866.
(23) De Silva, A.; Felix, N. M.; Ober, C. K. Molecular Glass Resists as High-Resolution Patterning Materials. *Adv. Mater.* **2008**, *20*, 3355−3361.
(24) Kudo, H.; Watanabe, D.; Nishikubo, T.; Maruyama, K.; Shimizu, D.; Kai, T.; Shimokawa, T.; Ober, C. K. A novel noria (water-wheel-like cyclic oligomer) derivative as a chemically amplified electron-beam resist material. *J. Mater. Chem.* **2008**, *18*, 3588−3592.
(25) André, X.; Lee, J. K.; De Silva, A.; Felix, N.; Ober, C. K.; Cao, H. B.; Deng, H.; Kudo, H.; Watanabe, D.; Nishikubo, T. Phenolic molecular glasses as resists for next-generation lithography. *Proc. SPIE* **2007**, *6519*, 65194B.
(26) Oizumi, H.; Matsunaga, K.; Kaneyama, K.; Santillan, J. J.; Shiraishi, G.; Itani, T. Performance of EUV molecular resists based on fullerene derivatives. *Proc. SPIE* **2011**, *7972*, 797209.
(27) Frommhold, A.; Yang, D. X.; McClelland, A.; Xue, X.; Ekinci, Y.; Palmer, R. E.; Robinson, A. P. G. Optimization of fullerene-based negative tone chemically amplified fullerene resist for extreme ultraviolet lithography. *Proc. SPIE* **2014**, *9051*, 905119.
(28) Yamamoto, H.; Kudo, H.; Kozawa, T. Study on resist performance of chemically amplified molecular resist based on noria derivative and calixarene derivative. *Proc. SPIE* **2014**, *9051*, 90511Z.
(29) Niina, N.; Kudo, H.; Oizumi, H.; Itani, T.; Nishikubo, T. Synthesis and property of noria (water-wheel like macrocycle) derivatives with pendant alkoxyl and adamantyl ester groups, and their application for extreme ultraviolet resist. *Thin Solid Films* **2013**, *534*, 459−464.
(30) Wang, X.; Tao, P.; Wang, Q.; Zhao, R.; Liu, T.; Hu, Y.; Hu, Z.; Wang, Y.; Wang, J.; Tang, Y.; Xu, H.; He, X. Trends in photoresist materials for extreme ultraviolet lithography: A review. *Mater. Today* **2023**, *67*, 299−319.
(31) Zhang, Y.; Yu, H.; Wang, L.; Wu, X.; He, J.; Huang, W.; Ouyang, C.; Chen, D.; Keshta, B. E. Advanced lithography materials: From fundamentals to applications. *Adv. Colloid Interface Sci.* **2024**, *329*, 103197.
(32) Wang, Y.; Chen, L.; Yu, J.; Guo, X.; Wang, S.; Yang, G. Negative-tone molecular glass photoresist for high-resolution electron beam lithography. *R. Soc. Open Sci.* **2021**, *8*, 202132.
(33) Chen, J.; Hao, Q.; Wang, S.; Li, S.; Yu, T.; Zeng, Y.; Zhao, J.; Yang, S.; Wu, Y.; Xue, C.; Yang, G.; Li, Y. Molecular Glass Resists Based on 9,9′-Spirobifluorene Derivatives: Pendant Effect and Comprehensive Evaluation in Extreme Ultraviolet Lithography. *ACS Appl. Polym. Mater.* **2019**, *1*, 526−534.
(34) Wang, Y.; Chen, J.; Zeng, Y.; Yu, T.; Guo, X.; Wang, S.; Allenet, T.; Vockenhuber, M.; Ekinci, Y.; Zhao, J.; Yang, S.; Wu, Y.; Yang, G.; Li, Y. Molecular Glass Resists Based on Tetraphenylsilane Derivatives: Effect of Protecting Ratios on Advanced Lithography. *ACS Omega* **2022**, *7*, 29266−29273.
(35) Hu, S.; Chen, J.; Yu, T.; Zeng, Y.; Yang, G.; Li, Y. Chemically Amplified Resist Based on Dendritic Molecular Glass for Electron Beam Lithography. *Chem. Res. Chin. Univ.* **2023**, *39*, 139−143.
(36) Hu, S.; Chen, J.; Yu, T.; Zeng, Y.; Wang, S.; Guo, X.; Yang, G.; Li, Y. A novel dual-tone molecular glass resist based on adamantane derivatives for electron beam lithography. *J. Mater. Chem. C* **2022**, *10*, 9858−9866.
(37) Frommhold, A.; Manyam, J.; Palmer, R. E.; Robinson, A. P. G. Fullerene-based spin-on-carbon hardmask. *Microelectron. Eng.* **2012**, *98*, 552−555.
(38) Cardineau, B. Molecular organometallic resists for EUV (MORE). In *Materials and Processes for Next Generation Lithography*; Robinson, A., Lawson, R., Eds.; Elsevier: Amsterdam, 2016; pp 377−420.
(39) Lim, G.; Lee, K.; Choi, S.; Yoon, H. J. Organometallic and coordinative photoresist materials for EUV lithography and related photolytic mechanisms. *Coord. Chem. Rev.* **2023**, *493*, 215307.
(40) Sharps, M. C.; Frederick, R. T.; Javitz, M. L.; Herman, G. S.; Johnson, D. W.; Hutchison, J. E. Organotin Carboxylate Reagents for Nanopatterning: Chemical Transformations during Direct-Write Electron Beam Processes. *Chem. Mater.* **2019**, *31*, 4840−4850.
(41) Wu, L.; Baljozovic, M.; Portale, G.; Kazazis, D.; Vockenhuber, M.; Jung, T.; Ekinci, Y.; Castellanos, S. Mechanistic insights in Zr- and Hf-based molecular hybrid EUV photoresists. *J. Micro/Nanolithogr., MEMS, MOEMS* **2019**, *18*, 1.
(42) Capitanio, D.; Yoshiki, M.; Lee, J. Metal ion removal from photoresist solvents. *Proc. SPIE* **1999**, *3678*, 684−688.
(43) Yu, T.; Ching, P.; Ober, C.; Deshpande, S.; Puligadda, R. Development of a Bond Contribution Model for Structure: Property Correlations in Dry Etch Studies. *Proc. SPIE* **2001**, *4345*, 945−951.
(44) Kunz, R. R.; Palmateer, S. C.; Forte, A. R.; Allen, R. D.; Wallraff, G. M.; DiPietro, R. A.; Hofer, D. C. Limits to Etch Resistance for 193-nm Single-Layer Resists. *Proc. SPIE* **1996**, *2724*, 365−376.
(45) Gokan, H.; Esho, S.; Ohnishi, Y. Dry Etch Resistance of Organic Materials. *J. Electrochem. Soc.* **1983**, *130*, 143−146.
(46) Argitis, P.; Vasilopoulou, M. A.; Gogolides, E.; Tegou, E.; Hatzakis, M.; Kollia, Z.; Cefalas, A. C. Etch Resistance Enhancement and Absorbance Optimization with Polyaromatic Compounds for the Design of 193 nm Photoresists. *Microelectron. Eng.* **1998**, *41−42*, 355−358.
(47) Gogolides, E.; Argitis, P.; Couladouros, E. A.; Vidali, V. P.; Vasilopoulou, M.; Cordoyiannis, G.; Diakoumakos, C. D.; Tserepi, A. Photoresist etch resistance enhancement using novel polycarbocyclic derivatives as additives. *J. Vac. Sci. Technol. B* **2003**, *21*, 141−147.
(48) Frisch, M. J.; Trucks, G. W.; Schlegel, H. B.; Scuseria, G. E.; Robb, M. A.; Cheeseman, J. R.; Scalmani, G.; Barone, V.; Petersson, G. A.; Nakatsuji, H.; Li, X.; Caricato, M.; Marenich, A. V.; Bloino, J.; Janesko, B. G.; Gomperts, R.; Mennucci, B.; Hratchian, H. P.; Ortiz, J. V.; Izmaylov, A. F.; Sonnenberg, J. L.; Williams-Young, D.; Ding, F.; Lipparini, F.; Egidi, F.; Goings, J.; Peng, B.; Petrone, A.; Henderson, T.; Ranasinghe, D.; Zakrzewski, V. G.; Gao, J.; Rega, N.; Zheng, G.; Liang, W.; Hada, M.; Ehara, M.; Toyota, K.; Fukuda, R.; Hasegawa, J.; Ishida, M.; Nakajima, T.; Honda, Y.; Kitao, O.; Nakai, H.; Vreven, T.; Throssell, K.; Montgomery, J. A., Jr.; Peralta, J. E.; Ogliaro, F.; Bearpark, M. J.; Heyd, J. J.; Brothers, E. N.; Kudin, K. N.; Staroverov, V. N.; Keith, T. A.; Kobayashi, R.; Normand, J.; Raghavachari, K.; Rendell, A. P.; Burant, J. C.; Iyengar, S. S.; Tomasi, J.; Cossi, M.; Millam, J. M.; Klene, M.; Adamo, C.; Cammi, R.; Ochterski, J. W.; Martin, R. L.; Morokuma, K.; Farkas, O.; Foresman, J. B.; Fox, D. J. *Gaussian 16*. A.03; Gaussian, Inc.: Wallingford CT, 2016.
(49) Grimme, S.; Ehrlich, S.; Goerigk, L. Effect of the damping function in dispersion corrected density functional theory. *J. Comput. Chem.* **2011**, *32*, 1456−1465.
(50) Weigend, F.; Ahlrichs, R. Balanced basis sets of split valence, triple zeta valence and quadruple zeta valence quality for H to Rn: Design and assessment of accuracy. *Phys. Chem. Chem. Phys.* **2005**, *7*, 3297−3305.
(51) Weigend, F. Accurate Coulomb-fitting basis sets for H to Rn. *Phys. Chem. Chem. Phys.* **2006**, *8*, 1057−1065.
(52) Yang, G.; Cong, X.; Guo, X.; Hu, R.; Wang, S. Fused ring aromatic hydrocarbon derivative, preparation method therefor, and use thereof in lithography. U.S. Patent 20,240,184,202 A1, 2023.
(53) Wang, Y.; Yuan, J.; Chen, J.; Zeng, Y.; Yu, T.; Guo, X.; Wang, S.; Yang, G.; Li, Y. A Single-Component Molecular Glass Resist Based on Tetraphenylsilane Derivatives for Electron Beam Lithography. *ACS Omega* **2023**, *8*, 12173−12182.
(54) Lee, C.-T.; Wang, M.; Gonsalves, K. E.; Yueh, W.; Roberts, J. M.; Younkin, T. R.; Henderson, C. L. Effect of PAG and matrix structure on PAG acid generation behavior under UV and high-energy radiation exposure. *Proc. SPIE* **2008**, *6923*, 69232F.

(55) Nakano, A.; Okamoto, K.; Yamamoto, Y.; Kozawa, T.; Tagawa, S.; Kai, T.; Nemoto, H. Dependence of Acid Yield on Acid Generator in Chemically Amplified Resist for Post-Optical Lithography. *Jpn. J. Appl. Phys.* **2005**, *44*, 5832.
(56) Kozawa, T.; Tagawa, S. Radiation Chemistry in Chemically Amplified Resists. *Jpn. J. Appl. Phys.* **2010**, *49*, 030001.
(57) Lakowicz, J. R. Advanced Topics in Fluorescence Quenching. In *Principles of Fluorescence Spectroscopy*, 3rd ed,; Springer: New York, 2006; pp 267−289.
(58) Moon, S.-Y.; Maekawa, Y.; Yoshida, M. Electron Beam-Induced Reactions of a Sulfonium Salt in the Solid State for Chemically Amplified Electron Beam Resists; Comparison with Photolytic Reactions. *J. Photopolym. Sci. Technol.* **2002**, *15*, 423−426.
(59) Kuznetsova, N. A.; Malkov, G. V.; Gribov, B. G. Photoacid generators. Application and current state of development. *Russ. Chem. Rev.* **2020**, *89*, 173−190.
(60) Grzeskowiak, S.; Kaminsky, J.; Gibbons, S.; Narasimhan, A.; Brainard, R. L.; Denbeaux, G. Electron trapping: a mechanism for acid production in extreme ultraviolet photoresists. *J. Micro/Nanolithogr., MEMS, MOEMS* **2018**, *17*, 033501.

https://doi.org/10.1021/acsomega.4c01044
ACS Omega 2024, 9, 37585−37595